22nd International Conference on Sustainable Energy Technologies
Kuala Lumpur, Malaysia, 13 to 15 August 2026 · ISBN 978-1-995850-00-9 · ISSN 2978-4387

CONFERENCE PAPER · POLICY & MANAGEMENT

Assessing the Impact of Transportation Infrastructure Development on Land Use/Land Cover Change and Urban Heat Island Dynamics in Benin City, Nigeria

Geraldine Nkechinyere Okeudo[1]*, Francis Ezinwanne Onuegbu[1]

[1] Department of Urban and Regional Planning, Abia State University, Uturu, Nigeria

RECEIVED 26 June 2026 · REVISED 10 July 2026 · ACCEPTED 18 July 2026
PRESENTED 13 to 15 August 2026 · PUBLISHED 23 November 2026

ABSTRACT

Transportation infrastructure development is a major driver of urban expansion and environmental transformation in rapidly growing cities of the Global South. This study examines the impact of transportation infrastructure development on land use/land cover (LULC) change and Urban Heat Island (UHI) dynamics in Benin City, Nigeria, between 2003 and 2025. Landsat 5 TM, Landsat 8 OLI/TIRS, and Landsat 9 OLI/TIRS imagery were analyzed using remote sensing and GIS techniques to derive Land Surface Temperature (LST), the Normalized Difference Vegetation Index (NDVI), and LULC classifications. A supervised Random Forest algorithm classified the study area into built-up areas, vegetation, bare surfaces, and water bodies, while Pearson correlation analysis assessed the relationship between NDVI and LST. Results indicate substantial land cover transformation, characterized by the expansion of transportation corridors and built-up areas, alongside declining vegetation cover and increasing bare surfaces. Mean LST increased from 16.39 °C in 2003 to 21.03 °C in 2025, reflecting intensified urban thermal conditions. NDVI analysis showed a decline in vegetation health and density, while a strong negative correlation between NDVI and LST was observed in 2015 ($r = -0.840$) and 2025 ($r = -0.842$), confirming the cooling effect of vegetation. Spatial analysis identified thermal hotspots concentrated in densely urbanized, transportation-dominated areas. The findings demonstrate that transportation-driven urban expansion significantly influences UHI intensity by altering land cover and surface thermal characteristics. The study underscores the need to integrate green infrastructure, climate-sensitive urban design, and sustainable transportation planning into urban development strategies to mitigate UHI effects and enhance environmental sustainability.

KEYWORDS Urban heat island (UHI), Transportation infrastructure, Land surface temperature (LST), Remote sensing, Benin City

1. Introduction

Urban areas across the Global South are undergoing rapid spatial transformation, driven largely by population growth, economic expansion, and infrastructure development. Among the key drivers of this transformation, transportation infrastructure plays a particularly influential role by reshaping land use patterns, redistributing human activities, and accelerating urban expansion. New road networks, highways, and transport corridors often act as catalysts for development, triggering the conversion of natural and peri-urban landscapes into built-up environments. While such developments enhance accessibility and economic productivity, they also introduce significant environmental consequences that are increasingly difficult to ignore. One of the most critical environmental outcomes associated with urban expansion is the modification of local thermal

* Corresponding author. Email address: geraldine.okeudo@abiastateuniversity.edu.ng (Geraldine Nkechinyere Okeudo)

© 2026 The Author(s).
Published by Caravel Press.

doi.org/10.65582/set.2026.036

conditions, commonly expressed through the Urban Heat Island (UHI) effect. The replacement of vegetated surfaces with impervious materials such as asphalt and concrete alters surface energy balance, reduces evapotranspiration, and increases heat storage capacity. As a result, urban areas tend to exhibit higher land surface temperatures compared to their rural surroundings, with implications for energy demand, thermal comfort, public health, and ecosystem stability (Zhou *et al.* 2018; Li *et al.* 2017). In rapidly urbanizing regions, these impacts are often intensified by unplanned growth and limited environmental regulation.

Land Surface Temperature (LST), derived from satellite thermal data, has become a widely used indicator for assessing urban thermal environments and quantifying UHI intensity. The integration of LST with land use/land cover (LULC) data enables a more comprehensive understanding of how spatial transformations influence urban climate systems. Recent studies have consistently shown that increases in built-up areas are associated with rising surface temperatures, whereas vegetation and water bodies contribute to localized cooling effects (Estoque *et al.* 2017; Guha *et al.* 2018). However, the role of transportation infrastructure as a mediating factor in this relationship remains insufficiently explored, particularly in developing country contexts. Vegetation dynamics, often represented by the Normalized Difference Vegetation Index (NDVI), further complicate the relationship between urban growth and thermal conditions. NDVI serves as a proxy for vegetation health and density and is frequently used to assess the cooling capacity of urban green spaces. Empirical evidence generally supports an inverse relationship between NDVI and LST, indicating that areas with higher vegetation cover tend to exhibit lower temperatures (Kafy *et al.* 2021; Sun *et al.* 2019). Nonetheless, the strength of this relationship varies spatially and temporally, especially in cities experiencing rapid infrastructural expansion, where vegetation loss may not occur uniformly.

In recent years, advances in geospatial technologies have improved the ability to analyze these complex interactions. Cloud-based platforms such as Google Earth Engine, along with machine learning and spatial modeling techniques, have enhanced the efficiency and accuracy of multi-temporal urban analyses (Amani *et al.* 2020; Tamiminia *et al.* 2020). Despite these methodological improvements, a significant proportion of existing studies has focused on large metropolitan areas, with relatively limited attention given to intermediate cities in Sub-Saharan Africa. Benin City, Nigeria, represents a compelling case study due to its rapid urban expansion and ongoing transportation infrastructure development. In recent decades, the city has experienced significant changes in road networks and urban form, leading to notable shifts in land use patterns. These transformations are likely to have important implications for local thermal environments, yet empirical studies explicitly linking transportation infrastructure, LULC change, and UHI dynamics in the city remain scarce. This gap limits the ability of planners and policymakers to develop targeted, climate-responsive urban strategies.

Furthermore, much of the existing literature tends to examine LST, NDVI, and LULC independently, without fully integrating the role of infrastructure development as a driving mechanism. There is therefore a need for a more holistic, multi-temporal approach that captures the interconnected nature of these variables and their evolution over time. Understanding these linkages is particularly important in the context of sustainable urban planning, where balancing infrastructure development with environmental resilience has become a central concern.

Against this backdrop, this study investigates the impact of transportation infrastructure development on land use/land cover change and Urban Heat Island dynamics in Benin City, Nigeria, over the period 2003–2025. Specifically, the study aims to: (i) analyze spatiotemporal changes in LULC, (ii) assess variations in land surface temperature, (iii) examine the relationship between LST and NDVI, and (iv) evaluate how transportation-driven urban expansion influences UHI patterns. By integrating remote sensing and GIS-based analysis, the study seeks to provide empirical evidence that supports more sustainable and climate-sensitive urban development strategies.

2. Methodology

2.1. Research Design and Analytical Framework

This study adopts an integrated geospatial analytical framework to investigate the impact of transportation infrastructure development on land use/land cover (LULC) dynamics and urban heat island (UHI) patterns. The approach combines remote sensing, GIS-based spatial analysis, and statistical modeling to evaluate both spatial and temporal changes.

The analytical workflow consists of four major components: (i) satellite data acquisition and pre-processing, (ii) LULC classification and change detection, (iii) land surface temperature (LST) retrieval and UHI mapping, and (iv) statistical and spatial analysis of relationships between infrastructure, vegetation, and thermal patterns. Such multi-layered frameworks are widely adopted in contemporary urban climate studies due to their ability to capture complex environmental interactions (Amani *et al.* 2020).

2.2. Data Sources and Description

2.2.1. Satellite Data

Multi-temporal Landsat imagery was acquired from the United States Geological Survey (USGS) Earth Explorer platform. The datasets used include:

- Landsat 5 TM (2003)
- Landsat 8 OLI/TIRS (2015)
- Landsat 9 OLI/TIRS (2025)

These datasets provide medium-resolution multispectral and thermal bands suitable for long-term environmental monitoring.

2.2.2. Ancillary Data

Additional datasets were incorporated to support spatial analysis:

- Road network and transportation infrastructure data
- Administrative boundary shapefiles
- High-resolution imagery for training and validation

The integration of ancillary datasets enhances the interpretation of spatial relationships between infrastructure development and environmental change.

2.3. Software, Tools, and Platforms

The study utilized a combination of cloud-based and desktop geospatial tools:

- Google Earth Engine (GEE): Data processing, image filtering, and index computation
- ArcGIS / QGIS: Spatial analysis, mapping, and visualization
- ENVI (optional): Image processing and classification support
- Microsoft Excel / SPSS: Statistical analysis and correlation modeling

GEE, in particular, has become a widely adopted platform for large-scale geospatial analysis due to its computational efficiency and access to extensive satellite archives (Tamiminia *et al.* 2020; Amani *et al.* 2020).

2.4. Image Pre-processing

To ensure consistency across datasets, all satellite images underwent standard pre-processing procedures, including:

- Radiometric correction
- Atmospheric correction
- Cloud masking using QA bands
- Image compositing
- Geometric alignment and reprojection

Surface reflectance products were used to minimize atmospheric distortions and improve the reliability of derived indices and thermal measurements. Proper pre-processing is essential for ensuring comparability across multi-temporal datasets (Guha *et al.* 2018).

2.5. Land Use/Land Cover Classification

2.5.1. Classification Scheme

LULC classification was performed into four major classes:

- Built-up areas
- Vegetation
- Bare surfaces
- Water bodies

2.5.2. Classification Method

A supervised machine learning approach using the Random Forest (RF) algorithm was employed. RF is preferred due to its robustness, high accuracy, and ability to handle non-linear relationships in remote sensing data. Training samples were generated using high-resolution imagery and existing land cover maps. The classifier was trained and applied within the GEE environment.

Recent studies confirm that Random Forest outperforms conventional classification techniques in urban environments (Kafy *et al.* 2021).

2.6. Accuracy Assessment

- Overall Accuracy (OA):

$$\mathrm{OA} = \frac{\sum_{i=1}^{n} X_{ii}}{N} \tag{1}$$

Where: X_{ii} = number of correctly classified pixels for class i; N = total number of pixels in the confusion matrix; n = number of classes.

- Kappa Coefficient (K):

$$K = \frac{N\sum X_{ii} - \sum \left(X_{i+} \cdot X_{+i}\right)}{N^2 - \sum \left(X_{i+} \cdot X_{+i}\right)} \tag{2}$$

Where: X_{ii} = correctly classified pixels; X_{i+} = total pixels in row i; X_{+i} = total pixels in column i; N = total number of observations.

2.7. Land Surface Temperature (LST) Retrieval

2.7.1. DN to Spectral Radiance

$$L_\lambda = M_L \times Q_{\text{cal}} + A_L \tag{3}$$

Where: L_λ = spectral radiance ($\text{W}\cdot\text{m}^{-2}\cdot\text{sr}^{-1}\cdot\mu\text{m}^{-1}$); M_L = radiance multiplicative scaling factor; A_L = radiance additive scaling factor; Q_{cal} = quantized calibrated pixel value (DN).

2.7.2. Radiance to Brightness Temperature (BT)

$$\text{BT} = \frac{K_2}{\ln\left(\frac{K_1}{L_\lambda} + 1\right)} \tag{4}$$

Where: BT = at-sensor brightness temperature (Kelvin); K_1, K_2 = thermal calibration constants (sensor-specific); L_λ = spectral radiance.

2.7.3. Proportion of Vegetation (Pv)

$$P_v = \left(\frac{\text{NDVI} - \text{NDVI}_{\text{min}}}{\text{NDVI}_{\text{max}} - \text{NDVI}_{\text{min}}}\right)^2 \tag{5}$$

Where: P_v = proportion of vegetation; $NDVI$ = normalized difference vegetation index; $NDVI_{\text{min}}$ = minimum NDVI value in the image; $NDVI_{\text{max}}$ = maximum NDVI value in the image.

2.7.4. Land Surface Emissivity (LSE)

$$\varepsilon = 0.004 \times P_v + 0.986 \tag{6}$$

Where: ε = land surface emissivity; P_v = proportion of vegetation.

2.7.5. Final Land Surface Temperature (LST)

$$\text{LST} = \frac{\text{BT}}{1 + \left(\frac{\lambda \cdot \text{BT}}{\rho}\right)\ln(\varepsilon)} \tag{7}$$

Where: LST = land surface temperature (Kelvin); BT = brightness temperature (Kelvin); λ = wavelength of emitted radiance ($\approx$ 10.8 μm for Landsat); $\rho = \frac{h \cdot c}{\sigma} = 1.438 \times 10^{-2} mK$; h = Planck's constant (6.626×10^{-34} Js); c = speed of light (2.998×10^8 m/s); σ = Boltzmann constant (1.38×10^{-23} J/K); ε = land surface emissivity.

2.8. Spectral Indices Computation

2.8.1. NDVI

$$\mathrm{NDVI} = \frac{\mathrm{NIR} - \mathrm{Red}}{\mathrm{NIR} + \mathrm{Red}} \tag{8}$$

Where: NIR = reflectance in near-infrared band; Red = reflectance in red band.

2.8.2. NDBI

$$\mathrm{NDBI} = \frac{\mathrm{SWIR} - \mathrm{NIR}}{\mathrm{SWIR} + \mathrm{NIR}} \tag{9}$$

Where: $SWIR$ = reflectance in shortwave infrared band; NIR = reflectance in near-infrared band.

2.8.3. NDWI

$$\mathrm{NDWI} = \frac{\mathrm{Green} - \mathrm{NIR}}{\mathrm{Green} + \mathrm{NIR}} \tag{10}$$

Where: $Green$ = reflectance in green band; NIR = reflectance in near-infrared band.

2.9. Urban Heat Island (UHI) Analysis

2.9.1. Surface Urban Heat Island Intensity (SUHII)

$$\mathrm{SUHII} = \mathrm{LST}_{\mathrm{urban}} - \mathrm{LST}_{\mathrm{rural}} \tag{11}$$

Where: $SUHII$ = surface urban heat island intensity; LST_{urban} = mean land surface temperature of urban areas; LST_{rural} = mean land surface temperature of rural reference areas.

2.9.2. Normalized UHI Index

$$\mathrm{UHI}_{\mathrm{norm}} = \frac{\mathrm{LST}_i - \mathrm{LST}_{\mathrm{min}}}{\mathrm{LST}_{\mathrm{max}} - \mathrm{LST}_{\mathrm{min}}} \tag{12}$$

Where: UHI_{norm} = normalized urban heat index; LST_i = pixel-level land surface temperature; LST_{min} = minimum LST value; LST_{max} = maximum LST value.

2.9.3. Thermal Hotspot Analysis (Z-score)

$$Z = \frac{X - \mu}{\sigma} \tag{13}$$

Where: Z = standardized hotspot value; X = LST of a given pixel; μ = mean LST of the study area; σ = standard deviation of LST.

2.10. Statistical Analysis

2.10.1. Pearson Correlation Coefficient

$$r = \frac{\sum (X - \bar{X})(Y - \bar{Y})}{\sqrt{\sum (X - \bar{X})^2 \sum (Y - \bar{Y})^2}} \tag{14}$$

Where: r = correlation coefficient; X = NDVI values; Y = LST values; $\bar{X}$, $\bar{Y}$ = mean values of NDVI and LST respectively.

2.10.2. Multiple Linear Regression Model

$$\text{LST} = \beta_0 + \beta_1 \text{NDVI} + \beta_2 \text{NDBI} + \epsilon \tag{15}$$

Where: LST = dependent variable (land surface temperature); β_0 = intercept; β_1, β_2 = regression coefficients; $NDVI$, $NDBI$ = independent variables; ϵ = error term.

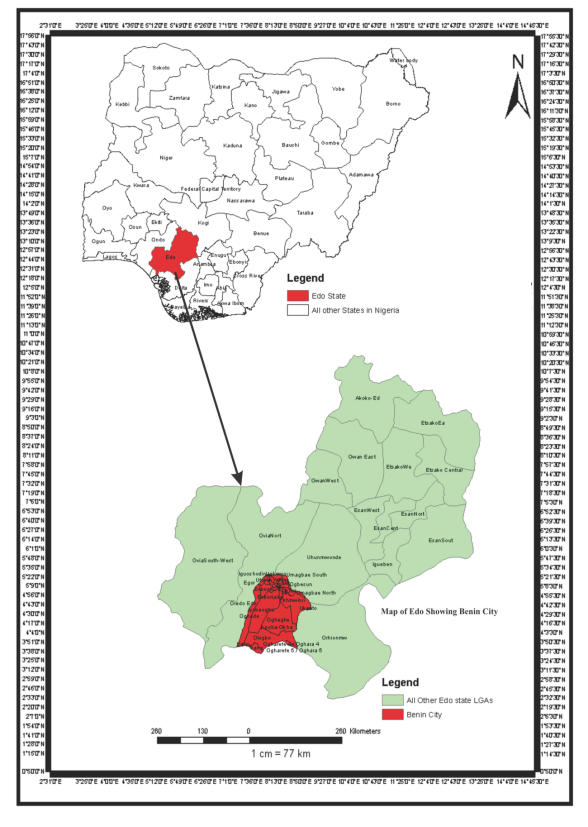

Figure 1. Map of the study area.

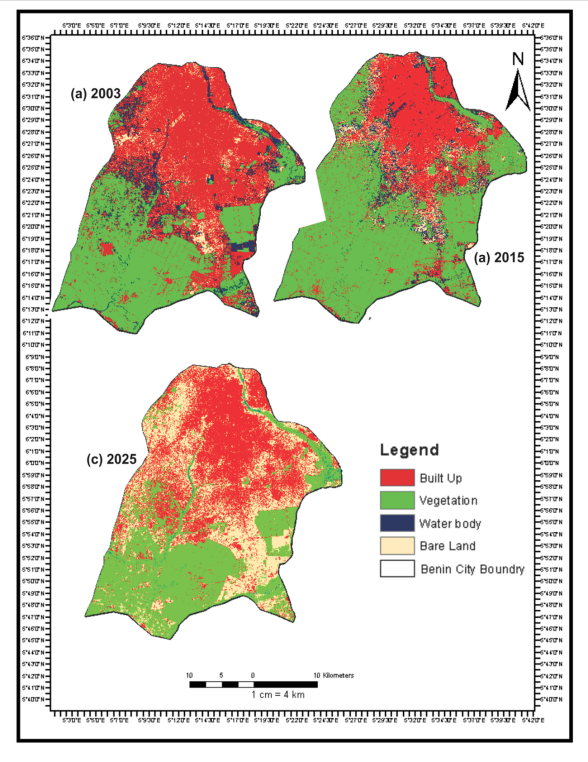

Figure 2. Benin City LULC 2003-2025.

Table 1. LULC results of Benin City 2003-2025.

Class	**LULC 2003**		**LULC 2015**		**LULC 2025**	
LULC	**Area km²**	**% Coverage**	**Area km²**	**% Coverage**	**Area km²**	**% Coverage**
Vegetation	475	39.3	691	57.1	414	34.21487603
Built Areas	563	46.6	356	29.4	413	34.1322314
Bare Surface	69	5.7	74	6.1	375	30.99173554
Water body	102	8.4	89	7.4	8	0.661157025
Total	**1209**	**100.0**	**1210**	**100**	**1210**	**100**

Table 2. LULC change detection 2002-2025.

Changes	**Area sq Km²**	**% Change**
Vegetation-Bare Land	62.585146	5.2
Vegetation-Built Up	43.527339	3.6
Vegetation-Vegetation	364.80261	30.2
Vegetation-Water Bodies	4.26599	0.4
Built Up-Bare Land	221.735156	18.3
Built Up-Built Up	323.015288	26.7
Built Up-Vegetation	17.611497	1.5
Built Up-Water Bodies	0.190475	0.0
Bare Surface-Bare Land	48.672705	4.0
Bare Surface-Built Up	20.083911	1.7
Bare Surface-Vegetation	0.625056	0.1
Bare Surface-Water Bodies	0.002477	0.0
Water body-Bare Land	41.590723	3.4

Table 2. (continued)

Changes	Area sq Km²	% Change
Water body-Built Up	26.05493	2.2
Water body-Vegetation	30.838688	2.6
Water body-Water Bodies	3.322312	0.3
Total	**1208.924303**	**100**

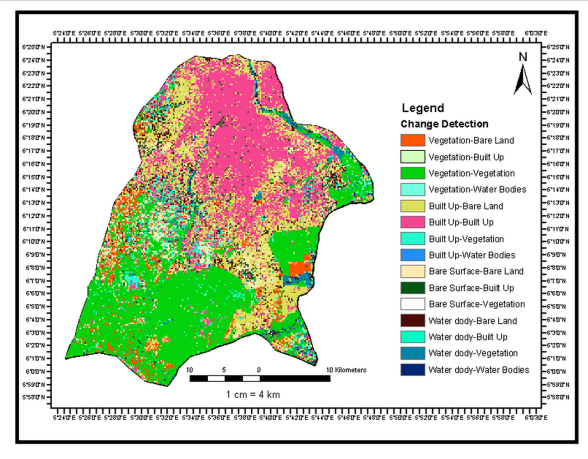

Figure 3. Benin City LULC change detection 2002-2025.

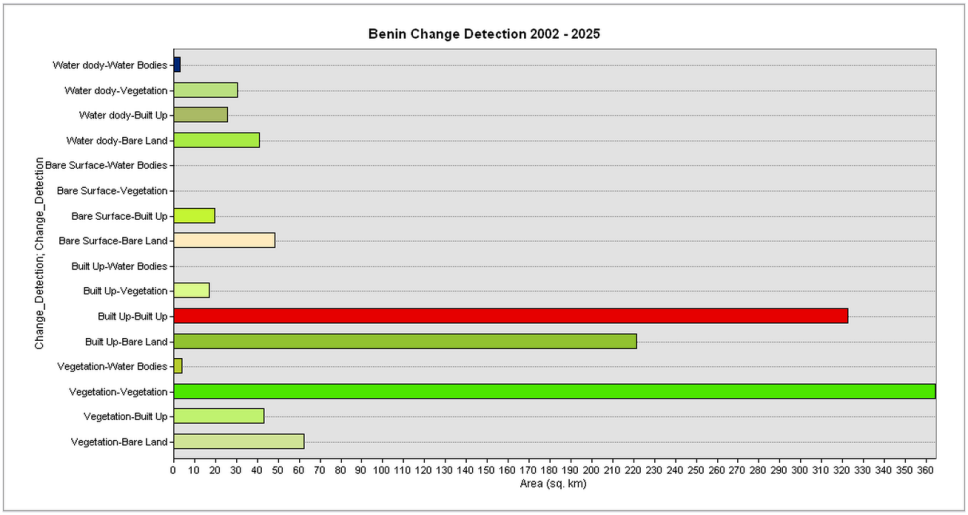

Figure 4. Graphical representation of Benin City 2003 – 2025 LULC change detection.

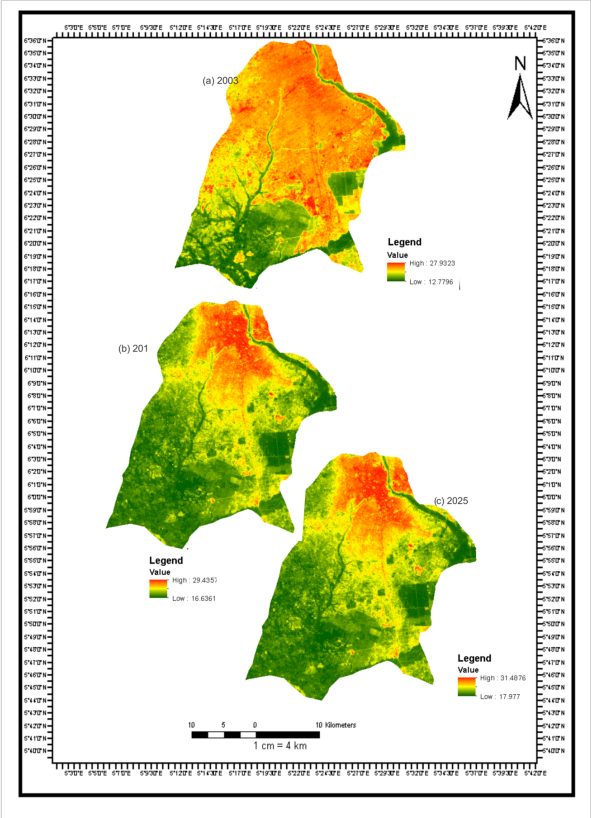

Figure 5. Land surface temperature of Benin City 2003-2025.

Table 3. LST of Benin City, 2003 - 2025.

Variables	LST 2003	LST 2015	LST 2025
Minimum	12.78	16.64	17.98
Maximum	27.93	29.44	31.49
Mean	16.386	19.53	21.028
Standard Deviation	1.57	1.92	2.0239

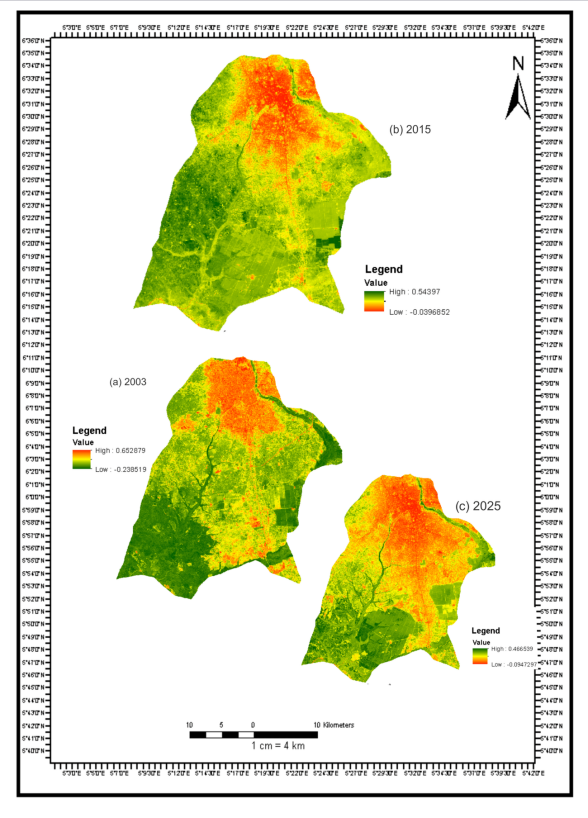

Figure 6. NDVI map of Benin City, 2003 - 2025.

Table 4. NDVI of Benin City, 2003 - 2025.

Variables	NDVI 2003	NDVI 2015	NDVI 2025
Minimum	−0.29	−0.039	0.095
Maximum	0.65	0.54	0.47
Mean	0.085	0.28	0.21
Standard Deviation	0.073	0.078	0.081

Table 5. Correlations between LST and NDVI 2003.

		LST	NDVI
LST	Pearson Correlation	1	.590**
	Sig. (2-tailed)		.000
	N	529	529
NDVI	Pearson Correlation	.590**	1
	Sig. (2-tailed)	.000	
	N	529	529

**. Correlation is significant at the 0.01 level (2-tailed).



Figure 7. Correlation between LST and NDVI 2003.

Table 6. Correlations between LST and NDVI 2015.

		LST	NDVI
LST	Pearson Correlation	1	-.840**
	Sig. (2-tailed)		.000
	N	529	529
NDVI	Pearson Correlation	-.840**	1
	Sig. (2-tailed)	.000	
	N	529	529

**. Correlation is significant at the 0.01 level (2-tailed).

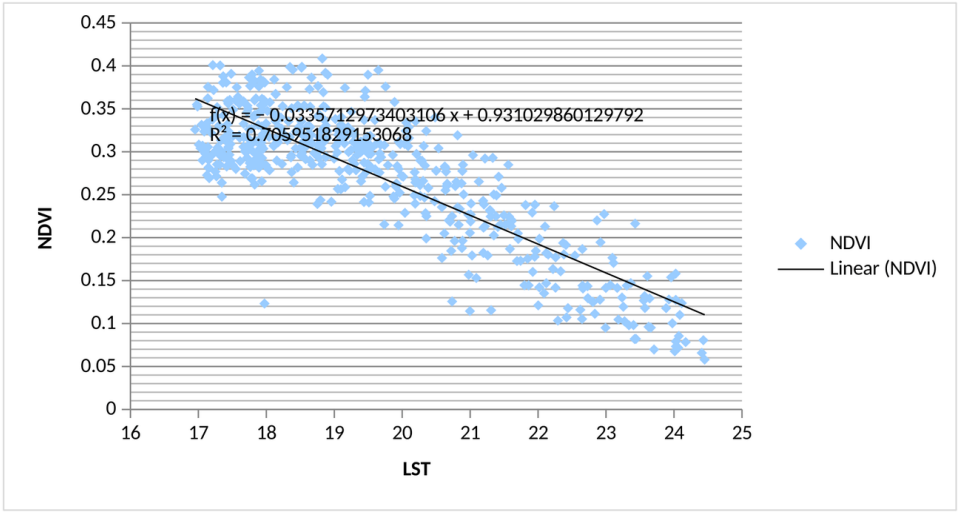

Figure 8. Correlation between LST and NDVI 2015.

Table 7. Correlations between LST and NDVI 2025.

		LST	NDVI
LST	Pearson Correlation	1	-.842**
	Sig. (2-tailed)		.000
	N	529	529
NDVI	Pearson Correlation	-.842**	1
	Sig. (2-tailed)	.000	
	N	529	529

**. Correlation is significant at the 0.01 level (2-tailed).

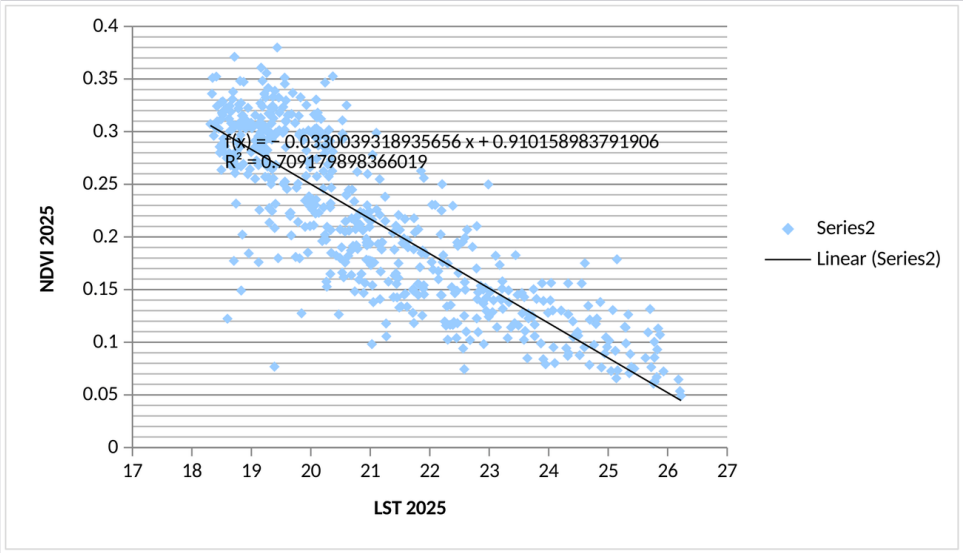

Figure 9. Correlation between LST and NDVI 2025.

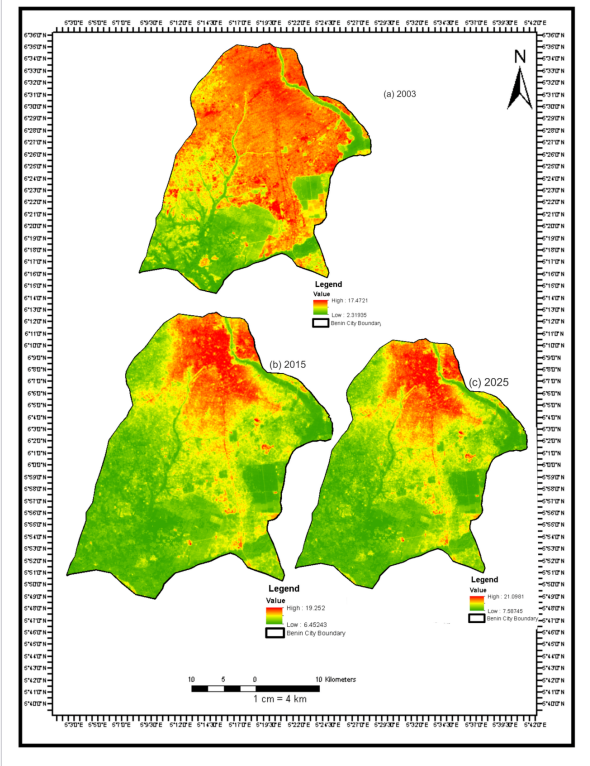

Figure 10. UHI map of Benin City 2003-2025.

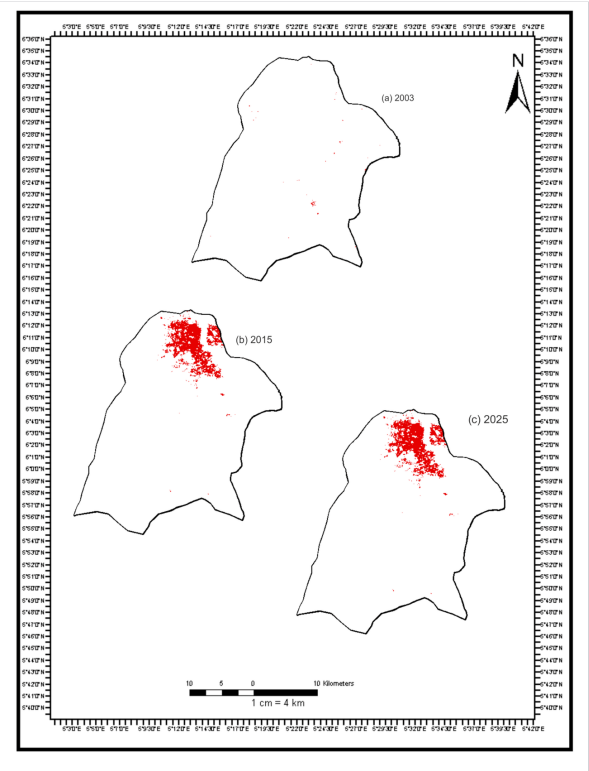

Figure 11. Urban hotspots map of Benin City 2003 – 2025.

3. Results and Discussion

3.1. Land Use/Land Cover (LULC) Dynamics (2003–2025)

The classification results (Tables 1 and 2; Figures 2–4) reveal substantial transformations in the spatial composition of land use/land cover within the study area over the study period. Built-up areas expanded markedly, primarily at the expense of vegetation and, to a lesser extent, bare land. This pattern reflects sustained urban growth and increased anthropogenic activity, consistent with trends observed in rapidly developing urban centers globally (Seto *et al.* 2012). Vegetation cover exhibited a noticeable decline in both spatial extent and continuity, indicating fragmentation of green spaces. Such fragmentation reduces ecological resilience and weakens the natural cooling capacity of urban landscapes. Conversely, the increase in impervious surfaces—such as asphalt and concrete—suggests intensified surface sealing, which has direct implications for thermal behavior. Similar findings have been reported in recent studies, where urban expansion is strongly linked to declining vegetation indices and increased thermal stress (Li *et al.* 2017).

The persistence of bare land in transitional zones further indicates ongoing development processes. These areas often represent construction sites or undeveloped parcels, which can exhibit high thermal variability due to exposed soil surfaces. Overall, the LULC results underscore a shift toward a more urbanized and thermally dynamic landscape.

3.2. Spatiotemporal Variation of Land Surface Temperature (LST)

The spatial distribution of LST (Figure 5; Table 3) demonstrates a heterogeneous thermal landscape, with distinct hotspots corresponding to built-up and sparsely vegetated areas. Over the study period, mean LST values showed moderate variability, with localized increases in high-density urban zones and relatively stable or declining temperatures in peripheral areas.

Interestingly, while urban expansion would typically correspond to a consistent increase in LST, the observed pattern suggests a more nuanced thermal response. Certain built-up areas exhibited stabilized or slightly reduced temperatures, potentially due to changes in building materials, urban

morphology, or increased adoption of reflective surfaces. This aligns with recent findings that urban thermal behavior is influenced not only by land cover type but also by material properties and urban design configurations (Zhou *et al.* 2018; Chakraborty *et al.* 2019).

High-temperature clusters were predominantly concentrated in zones characterized by dense infrastructure and limited vegetation cover. In contrast, areas with residual vegetation or proximity to water bodies exhibited relatively lower LST values, highlighting the moderating influence of natural elements.

3.3. NDVI Patterns and Vegetation Dynamics

The NDVI analysis (Figure 6; Table 4) indicates a general decline in vegetation health and density across the study area. High NDVI values were largely confined to isolated patches, while moderate-to-low values became increasingly widespread over time. This trend reflects both the reduction in vegetation cover and the degradation of existing green spaces.

The spatial correspondence between NDVI and LULC patterns reinforces the role of vegetation as a critical component of urban environmental quality. Areas that retained higher NDVI values consistently exhibited lower surface temperatures, supporting the well-established cooling effect of vegetation through evapotranspiration and shading.

However, the NDVI decline was not uniform, suggesting that local land management practices and micro-environmental conditions play a significant role in shaping vegetation dynamics. These variations highlight the importance of site-specific interventions in urban greening strategies.

3.4. Relationship between LST and NDVI

The statistical relationship between LST and NDVI (Tables 5–7; Figures 7–9) reveals a generally inverse correlation, indicating that areas with higher vegetation density tend to exhibit lower surface temperatures. This finding is consistent with a wide body of recent literature emphasizing the cooling benefits of urban vegetation (Guo *et al.* 2015).

Nevertheless, the strength of this relationship was found to vary spatially and temporally. In some highly urbanized zones, the correlation weakened, suggesting that vegetation alone may not be sufficient to offset the thermal effects of dense infrastructure. This observation supports the argument that urban heat dynamics are governed by multiple interacting factors, including surface materials, urban geometry, and anthropogenic heat emissions.

Moreover, the presence of bare land and transitional surfaces introduced additional complexity into the LST–NDVI relationship. These surfaces can exhibit high temperatures despite low vegetation indices, thereby influencing overall correlation patterns. The findings therefore highlight the limitations of relying solely on NDVI as a predictor of urban thermal conditions.

3.5. Urban Heat Island (UHI) Intensity Analysis

The analysis of UHI intensity (Figures 10 and 11) indicates a spatially differentiated pattern, with pronounced heat island effects in densely built-up areas. However, contrary to conventional expectations, the overall UHI intensity exhibited a slight decline over the study period. This unexpected trend suggests the influence of additional moderating factors beyond vegetation cover. Possible explanations include changes in urban surface materials, increased surface reflectivity, or spatial redistribution of heat due to evolving urban configurations. Recent studies have similarly reported that UHI intensity does not always increase linearly with urbanization, particularly when adaptive measures or structural changes are introduced.

The reduction in UHI intensity may also be linked to the dispersion of urban growth into peripheral areas, thereby reducing thermal concentration in the urban core. This spatial redistribution effect highlights the importance of considering urban form and expansion patterns in UHI analysis.

3.6. Integrated Discussion

The combined evidence from Tables 1–7 and Figures 2–11 demonstrates that the study area experienced significant land surface transformation, accompanied by complex thermal responses. While vegetation loss would typically lead to increased temperatures, the observed patterns indicate that urban thermal dynamics are influenced by a broader set of interacting factors. The findings align with recent research emphasizing that UHI is not solely a function of vegetation decline but also reflects the combined effects of land cover composition, surface materials, and urban morphology (Chakraborty *et al.* 2019). The weakening of the NDVI–LST relationship in certain areas further reinforces the need for multi-dimensional approaches to urban climate analysis.

From a planning perspective, the results suggest that effective UHI mitigation requires more than increasing vegetation cover. While urban greening remains essential, it should be complemented by strategies addressing surface materials, spatial configuration, and land-use planning. Approaches such as cool roofing, permeable surfaces, and optimized urban layouts can significantly enhance thermal regulation. This study contributes to the growing body of evidence that urban thermal environments are shaped by complex, context-specific interactions. By integrating LULC, LST, and NDVI analyses, it provides a more comprehensive understanding of urban heat dynamics and offers valuable insights for climate-responsive urban planning.

4. Conclusion, Policy Implications, and Recommendations

4.1. Conclusion

This study examined the spatiotemporal dynamics of land use/land cover (LULC), land surface temperature (LST), and Urban Heat Island (UHI) intensity over the period 2003–2025 using an integrated remote sensing and GIS-based approach. The findings, as presented in Tables 1–7 and Figures 2–11, demonstrate that the study area has undergone substantial landscape transformation characterized by continuous expansion of built-up surfaces and a corresponding decline in vegetation cover. The LST analysis revealed a heterogeneous thermal pattern, with higher temperatures concentrated in densely urbanized zones and relatively lower temperatures in areas with residual vegetation and open spaces. Although the general expectation is that urban expansion leads to intensified thermal conditions, the results indicate a more complex response, with localized cooling trends and a slight reduction in overall UHI intensity. This suggests that urban thermal environments are not solely controlled by vegetation loss but are shaped by the interaction of multiple factors, including surface materials, spatial configuration, and land-use restructuring.

The NDVI–LST relationship confirmed the cooling role of vegetation; however, the variability in correlation strength across space and time highlights the limitations of single-factor analysis. In highly urbanized areas, the reduced influence of vegetation suggests that additional mechanisms—such as built-form characteristics and anthropogenic heat—play a significant role in determining thermal conditions. These findings are consistent with recent studies emphasizing the multidimensional nature of urban heat dynamics (Zhou *et al.* 2018). The study provides empirical evidence that urban thermal behavior is governed by complex and context-specific interactions between land cover, urban morphology, and environmental processes. The integrated analytical framework adopted in this research offers a more comprehensive understanding of these dynamics and contributes to advancing urban climate studies, particularly in medium-sized and transitioning urban environments.

4.2. Policy Implications

The findings of this study have important implications for urban planning, environmental management, and climate adaptation policies.

First, the observed decline in vegetation cover and its impact on thermal regulation underscores the need for stronger urban greening policies. However, the results also indicate that vegetation

alone is insufficient to mitigate urban heat effectively. This calls for a shift from conventional greening approaches toward integrated urban climate planning that combines green infrastructure with material and structural interventions. Second, the spatial variability of LST and UHI intensity highlights the importance of location-specific planning strategies. Urban policies should prioritize hotspot areas identified in Figure 5 and Figure 11 for targeted interventions, such as increasing tree canopy cover, introducing green roofs, and enhancing urban ventilation corridors. Recent studies have emphasized that spatially explicit strategies are more effective than uniform approaches in addressing urban heat challenges (Chakraborty *et al.* 2019). Third, the role of impervious surfaces in amplifying thermal conditions suggests the need for regulating construction materials and promoting the adoption of high-albedo and permeable surfaces. Policies encouraging cool pavements and reflective roofing materials can significantly reduce heat absorption and improve urban thermal comfort (Zhou *et al.* 2018). Finally, the findings highlight the importance of integrating geospatial technologies into urban planning processes. Continuous monitoring of LULC and LST using remote sensing can support evidence-based decision-making and enable proactive responses to emerging thermal risks.

4.3. Recommendations

Based on the results and their implications, the following recommendations are proposed:

1. **Integrated Urban Greening Strategies** Urban planning authorities should move beyond isolated tree-planting initiatives and adopt comprehensive green infrastructure systems. This includes urban parks, green corridors, and vertical greening, which collectively enhance thermal regulation and ecological connectivity.
2. **Adoption of Climate-Responsive Urban Design** Building regulations should incorporate climate-sensitive design principles, including optimized building orientation, spacing, and ventilation pathways. Such measures can improve airflow and reduce heat accumulation in dense urban areas.
3. **Promotion of Cool and Permeable Surfaces** The use of reflective and permeable materials in roads, pavements, and rooftops should be encouraged through policy incentives and building codes. These materials help reduce surface temperatures and improve urban resilience to heat stress.
4. **Protection and Restoration of Vegetation** Existing green spaces should be protected from further encroachment, while degraded areas should be rehabilitated through afforestation and landscape restoration programs. Maintaining vegetation continuity is essential for sustaining its cooling benefits.
5. **Spatially Targeted Heat Mitigation Measures** Intervention efforts should focus on identified thermal hotspots (Figures 5 and 11), where the intensity of UHI is highest. Tailored strategies in these areas will yield more effective outcomes than generalized city-wide measures.
6. **Integration of Remote Sensing in Urban Management** Government agencies and planning institutions should institutionalize the use of satellite data and GIS tools for continuous monitoring of urban environmental conditions. This will enhance the capacity for adaptive and data-driven planning.
7. **Future Research Directions** Further studies should incorporate additional variables such as surface albedo, anthropogenic heat emissions, and socio-economic factors to better understand the drivers of urban heat dynamics. The application of advanced modeling techniques, including machine learning and spatial regression, is also recommended to improve predictive accuracy.

Declarations

Author contributions. Geraldine Nkechinyere Okeudo: Writing (original draft), Data curation, Formal analysis, Investigation, Methodology, Conceptualization. Francis Ezinwanne Onuegbu: Writing (review and editing).

Funding. This research received no specific funding.

Conflicts of interest. The authors declare no competing interests.

Data availability. The data that support the findings of this study are available from the corresponding author upon reasonable request.

References

Amani, Meisam; Ghorbanian, Arsalan; Ahmadi, Seyed Ali; Kakooei, Mohammad; Moghimi, Armin; Mirmazloumi, S. Mohammad; Moghaddam, Sayyed Hamed Alizadeh; Mahdavi, Sahel; Ghahremanloo, Masoud; Parsian, Saeid; Wu, Qiusheng; Brisco, Brian (2020) 'Google Earth Engine Cloud Computing Platform for Remote Sensing Big Data Applications: A Comprehensive Review', *IEEE Journal of Selected Topics in Applied Earth Observations and Remote Sensing*, 13, pp. 5326-5350. Available at: https://doi.org/10.1109/jstars.2020.3021052

Chakraborty, T.; Hsu, A.; Manya, D.; Sheriff, G. (2019) 'Disproportionately higher exposure to urban heat in lower-income neighborhoods: a multi-city perspective', *Environmental Research Letters*, 14(10), pp. 105003. Available at: https://doi.org/10.1088/1748-9326/ab3b99

Estoque, Ronald C.; Murayama, Yuji; Myint, Soe W. (2017) 'Effects of landscape composition and pattern on land surface temperature: An urban heat island study in the megacities of Southeast Asia', *Science of The Total Environment*, 577, pp. 349-359. Available at: https://doi.org/10.1016/j.scitotenv.2016.10.195

Guha, Subhanil; Govil, Himanshu; Dey, Anindita; Gill, Neetu (2018) 'Analytical study of land surface temperature with NDVI and NDBI using Landsat 8 OLI and TIRS data in Florence and Naples city, Italy', *European Journal of Remote Sensing*, 51(1), pp. 667-678. Available at: https://doi.org/10.1080/22797254.2018.1474494

Guo, Guanhua; Wu, Zhifeng; Xiao, Rongbo; Chen, Yingbiao; Liu, Xiaonan; Zhang, Xiaoshi (2015) 'Impacts of urban biophysical composition on land surface temperature in urban heat island clusters', *Landscape and Urban Planning*, 135, pp. 1-10. Available at: https://doi.org/10.1016/j.landurbplan.2014.11.007

Kafy, Abdulla-Al; Dey, Nataraj Narayan; Al Rakib, Abdullah; Rahaman, Zullyadini A.; Nasher, N. M. Refat; Bhatt, Abhishek (2021) 'Modeling the relationship between land use/land cover and land surface temperature in Dhaka, Bangladesh using CA-ANN algorithm', *Environmental Challenges*, 4, pp. 100190. Available at: https://doi.org/10.1016/j.envc.2021.100190

Li, Xiaoma; Zhou, Yuyu; Asrar, Ghassem R.; Imhoff, Marc; Li, Xuecao (2017) 'The surface urban heat island response to urban expansion: A panel analysis for the conterminous United States', *Science of The Total Environment*, 605-606, pp. 426-435. Available at: https://doi.org/10.1016/j.scitotenv.2017.06.229

Seto, Karen C.; Güneralp, Burak; Hutyra, Lucy R. (2012) 'Global forecasts of urban expansion to 2030 and direct impacts on biodiversity and carbon pools', *Proceedings of the National Academy of Sciences*, 109(40), pp. 16083-16088. Available at: https://doi.org/10.1073/pnas.1211658109

Sun, Ranhao; Lü, Yihe; Yang, Xiaojun; Chen, Liding (2019) 'Understanding the variability of urban heat islands from local background climate and urbanization', *Journal of Cleaner Production*, 208, pp. 743-752. Available at: https://doi.org/10.1016/j.jclepro.2018.10.178

Tamiminia, Haifa; Salehi, Bahram; Mahdianpari, Masoud; Quackenbush, Lindi; Adeli, Sarina; Brisco, Brian (2020) 'Google Earth Engine for geo-big data applications: A meta-analysis and systematic review', *ISPRS Journal of Photogrammetry and Remote Sensing*, 164, pp. 152-170. Available at: https://doi.org/10.1016/j.isprsjprs.2020.04.001

Zhou, Decheng; Xiao, Jingfeng; Bonafoni, Stefania; Berger, Christian; Deilami, Kaveh; Zhou, Yuyu; Frolking, Steve; Yao, Rui; Qiao, Zhi; Sobrino, José A. (2018) 'Satellite Remote Sensing of Surface Urban Heat Islands: Progress, Challenges, and Perspectives', *Remote Sensing*, 11(1), pp. 48. Available at: https://doi.org/10.3390/rs11010048

HOW TO CITE THIS PAPER

Okeudo, G. N. and Onuegbu, F. E. (2026). Assessing the Impact of Transportation Infrastructure Development on Land Use/ Land Cover Change and Urban Heat Island Dynamics in Benin City, Nigeria. In: *Proceedings of the 22nd International Conference on Sustainable Energy Technologies (SET2026)*, Kuala Lumpur, Malaysia, 13 to 15 August 2026. Caravel Press, pp. 436–454. ISBN 978-1-995850-00-9. ISSN 2978-4387. https://doi.org/10.65582/set.2026.036

COPYRIGHT AND LICENCE

© 2026 The Author(s). This is an open access paper distributed under the terms of the Creative Commons Attribution (CC BY 4.0) licence, which permits unrestricted use, distribution and reproduction in any medium, provided the original work is properly cited.

WSSET World Society of Sustainable Energy Technologies Organised by the World Society of Sustainable Energy Technologies. Published by Caravel Press.